Colloid Polym Sci (2003) 282: 110–118
DOI 10.1007/s00396-003-0900-7

ORIGINAL CONTRIBUTION

Yuxia Luan
Guiying Xu
Guoliang Dai
Zhiwei Sun
Hua Liang

The interaction between poly(vinylpyrrolidone) and reversed micelles of water/AOT/*n*-heptane

Received: 29 August 2002
Accepted: 4 March 2003
Published online: 9 May 2003

Y. Luan · G. Xu (✉) · H. Liang
Key Laboratory for Colloid & Interface Chemistry of Education Ministry, Shandong University, 250100 Jinan, China
E-mail: xuguiying@sdu.edu.cn
Fax: +86-531-8564750

G. Dai · Z. Sun
National Microgravity Laboratory, Institute of Mechanics, Chinese Academy of Sciences, 100080 Beijing, China

Abstract. The interactions between poly(vinylpyrrolidone) (PVP) and the reversed micelles composed of water, AOT, and *n*-heptane are investigated with the aid of phase diagram, measurements of conductivity and viscosity, Fourier transform infrared (FTIR) spectrum, and dynamic light scattering (DLS). The phase diagrams of water/AOT/heptane in the presence of and absence of PVP are given. The conductivity of the water/AOT/heptane reversed micelle without PVP initially increases and then decreases with the increase of water content, ω_0 (the molar ratio of water to AOT), while the plots of conductivity (κ) versus ω_0 of the reversed micelle in the presence of PVP depend on the PVP concentrations. The plot of κ versus ω_0 with 2.0%wt PVP is similar to that without PVP. Only the $\omega_{0,max}$ (the water content that the maximum conductivity corresponds to) is larger than that without PVP. Nevertheless, the conductivity of the reversed micelle containing more than 4%wt PVP always rises with the increase of the water content in the measured range. The DLS results indicate that the hydrodynamic radius (R_h) in the presence and absence of PVP rises with the increase of ω_0. The plots with PVP and without PVP have almost the same value when $\omega_0 < 17$; and after that, it quickly increases with the increase of ω_0. It is interesting to find that there is almost no effect of the PVP concentration on the viscosity and R_h of the reversed micelle at $\omega_0 = 15$. The FTIR results suggest that the contents of SO_3^--bound water and Na^+-bound water both decrease with PVP added, while the content of the bulky-like water increases. However, the trapped water in the hydrophobic chain of the surfactant is nearly unaffected by PVP. It is also found from the FTIR that the carbonyl group stretching vibration of AOT is fitted into two sub-peaks, which center at 1740 and 1729 cm^{-1}, corresponding to the *trans* and *cis* conformations of AOT, respectively.

Keywords Sodium bis(2-ethylhexyl)sulfosuccinate · AOT · Poly(vinylpyrrolidone) · PVP · Interaction

Introduction

The hydration of a solution of amphiphilic molecules in an apolar solvent can lead to the formation of three-dimensional structures known as reversed micelles [1, 2, 3]. AOT is a widely used surfactant with a double hydrophobic chain. It can form a microemulsion without adding any cosurfactants, and the microemulsion composed of AOT can accommodate a large amount of water. In addition, the size of the droplet increases with

the increase of water content [4, 5]. The microemulsions formed by AOT are widely used as microreactors for aqueous phase reactions [3, 6, 7]. It is also used in the preparation of nanometer particles, in the emulsification polymerization and biological catalysis [8]. According to the accepted reviews [9, 10], the water in the reversed micelles can be divided into at least two kinds: polar head hydration water ("bound" water) and bulk-like water ("free" water). The bound water has some unusual properties, such as high microviscosity, no freezing point, and blocking of the formation of hydrogen bonds [1]. The water in a reversed micelle is similar to the water in a biomembrane in many aspects [11], and hence much attention has been paid to the state and structure of the water in reversed micelles and microemulsions [12, 13, 14, 15, 16, 17]. People hope to mimic biomembranes and to disclose the biological physics and biological chemistry phenomena by investigating the water state in the reversed micelle and microemulsion. Much work has been done on the study of interactions between the water-soluble polymers and the reversed micelles, for example, the effects of the polymer on the size, structure and physical chemical properties of the reversed micelles [18, 19, 20, 21, 22]. However, general features of the interaction between PVP and AOT reversed micelles are still unclear.

In our previous work, we have studied the interaction between PVP and AOT in aqueous solution by means of surface tension and computer simulation [23]. The present paper aims to study the interactions between PVP and AOT reversed micelles with the use of the phase diagram, conductivity, viscosity, FTIR, and dynamic light scattering (DLS).

Experimental section

Materials

AOT was purchased from Fluka. *n*-Heptane was purchased from Shanghai Chemical Company (China). The PVP (K30 and K90) were bought from Beijing Chemical Reagent Company (China) and dried in the vacuum drier before use. The purity of the polymer was higher than 99% in weight. The content of the monomer residue and the sulfate residue were both lower than 0.1%wt.The water used to prepare the solution in the experiment was distilled three times.

Instruments

The conductivity instrument (model DDS-11A) used in our experiment is the product of the Second Analysis Instrumental Corporation of Shanghai. The constant of the cell is 1.05. The Ubbelohde viscometer was made in Shandong University. FTIR was carried out with FTS-165 (Biorad) under 2 cm^{-1} resolutions and 64 scanning. The measurements of DLS have been performed with a standard multi-angle spectrometer (the product of Brookhaven Instruments, USA); intensity correlations were processed through the BI-9000 correlator. An Argon-ion laser was used as the light source.

Experimental method

Phase diagram

The solutions of AOT and heptane with different ratios in weight are prepared, and the water is gradually injected into the solution under stirring. The solution is observed with the naked eye. The lamellar liquid crystal and hexagonal liquid crystal are determined with the polarimeter. The weight corresponding to the point that the solution becomes turbid or clear is written down, and then the ternary phase diagram is drawn by calculating the weight percentage of water in the total weight. According to the above method, the pseudo-ternary phase diagram can be also drawn when water is replaced by a 2.0%wt PVP-K30 solution.

Preparation of the microemulsion

AOT solution is obtained by dissolving AOT in the required amount of heptane to give 0.1 mol L^{-1}. The water or PVP-K30 aqueous solution is injected into the AOT solution to obtain the required system.

Measurements of the viscosity and conductivity

The viscosities of the reversed micelles containing different contents of water and different concentrations of PVP are measured with the Ubbelohde viscometer. The required solutions are prepared as described above and the measurement of conductivity is carried out on a DDS-11A conductivity instrument. All the experiments are performed at a temperature of 30.0 ± 0.1 °C.

Dynamic light scattering measurements

DLS measurements are performed using a frequency-stabilizing argon ion laser emitting vertically polarized light at 488 nm. The scattering cells are immersed in a thermostated bath of index-matching liquid (decalin) (to match the refractive index of glass). The measurements are performed at a scattering angle of 90º and the temperature is always controlled at 30.0 ± 0.1 °C.

The data analysis is according to reference [24].

Measurements of FTIR

In order to quantify the components of the hydroxyl and carbonyl stretching bands and their changes with polymer contents, the spectra have been subjected to a deconvolution process in Gaussion bands [17].

The measurements of FTIR are carried out as described in reference [25].

Results and discussion

The phase diagram

A phase diagram can provide a clear picture regarding the state of a system of certain composition [26, 27]. The phase diagrams of water (or PVP-K30 aqueous solution)/AOT/*n*-heptane are shown in Fig. 1. In this experiment the phase diagram with 2.0%wt PVP-K30 is used as an example for studying the effect of PVP on the phase diagram.

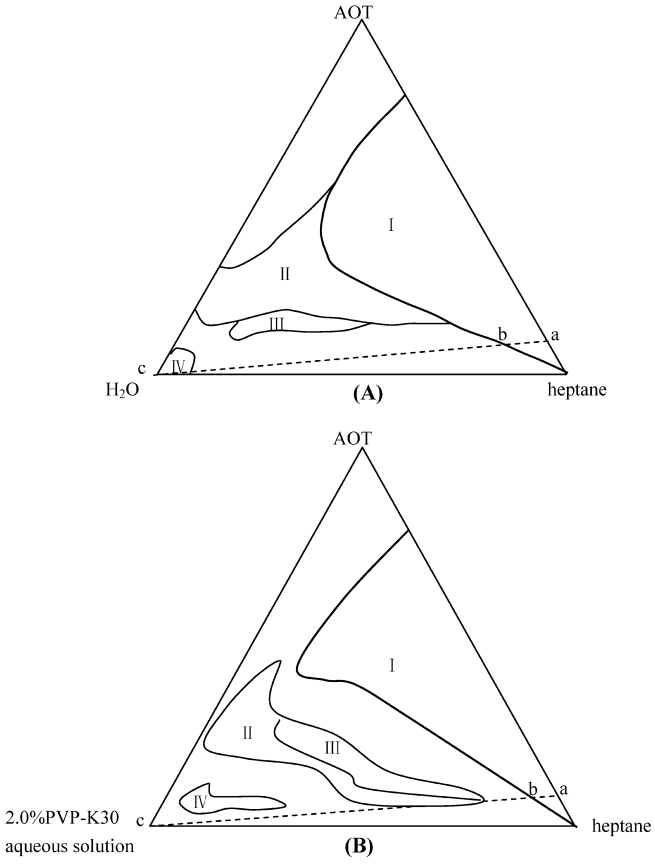

Fig. 1A–B Phase diagrams composed of H_2O, AOT, and *n*-heptane **A** with and **B** without PVP-K30

The regions of I, II, III, and IV represent the reversed micelle, the liquid crystal, the bicontinuous phase, and the O/W microemulsion, respectively. The dashed line refers to the 0.1 mol L^{-1} AOT solution studied in this paper with the water content increasing from a to c. The regions of the reversed micelle and the liquid crystal in the presence of PVP-K30 are both smaller than those in its absence, while the bicontinuous region is larger in the presence of PVP than in its absence. Only the reversed micelle region without PVP is similar to that of the water/AOT/isooctane system [19]. Also, it can be seen from the figure that the region of O/W microemulsion is further from the water acme in the presence of PVP.

Conductivities of the reversed micelles in the presence of different concentrations of PVP-K30

The curves shown in Fig. 2 are variations of the conductivity as a function of ω_0 for reversed micelles with different PVP-K30 concentrations. The conductivity of the reversed micelle without PVP initially increases and then decreases with the increase of ω_0; at $\omega_0 \approx 15$ the conductivity reaches its maximum. This result is caused by two effects. On the one hand, at small values of ω_0

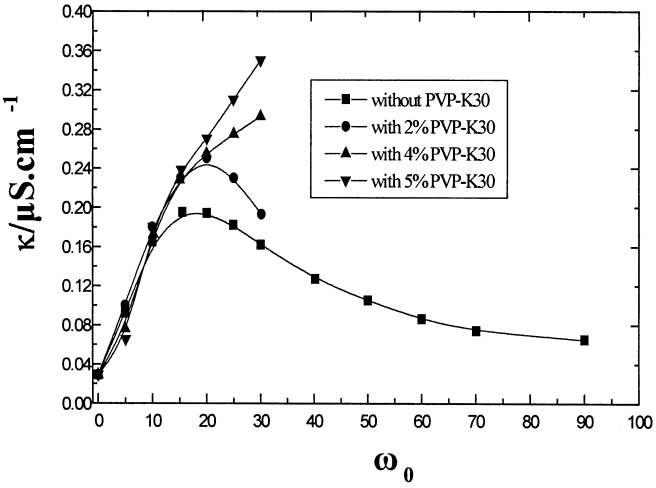

Fig. 2 Variation of conductivity with ω_0 of the reversed micelle

(the reversed micelle region) an increase of water content induces a better exchange of surfactant molecules between the micelles, and hence improves the conductivity due to the better mobility of the charged surfactant molecules. On the other hand, the addition of water dilutes the systems, which results in a decrease of the concentration of the conducting species [26]. The first effect is dominant at $\omega_0 < 15$, while the second effect is decisive at $\omega_0 > 15$. Thus, the conductivity initially increases and then decreases with the increase of ω_0. It is also observed that different concentrations of the polymer have different effects on the conductivity of the microemulsion. The plot of conductivity (κ) against ω_0 in the presence of 2.0% PVP-K30 is similar to that of the PVP-free system; only the value of $\omega_{0,max}$ becomes larger, $\omega_{0,max} \approx 20$. At the same time, the conductivities of the reversed micelle at $W_{PVP} \geq 4.0\%$ have no maximum values in the investigated ω_0 range. It is found that the reversed micelle becomes turbid when $\omega_0 > 30$ for the $W_{PVP} \geq 4.0\%$ system during the experimental course. The conductivity of reversed micelles is almost unaffected by PVP-K30 when ω_0 is below 10; while the conductivity in the presence of PVP-K30 is larger than that in its absence when $\omega_0 > 10$. This indicates a strong interaction between the polymer and the reversed micelles as described in the literature [19]. The attracting interaction between the reversed micelles increases with added water-soluble polymer. Similar results were also found by several groups [28, 29, 30] in the investigation of the effect of PEO and cytochrome C on the microemulsion composed of water, AOT, and isooctane.

Dynamic light scattering

Light scattering is a widely known experimental tool used to investigate the interaction between polymers and

surfactants because it is sensitive to the existence of large complexes [24, 31, 32]. Figure 3 shows the dependence of the hydrodynamic radius (R_h) of the reversed micelle on ω_0 in the presence of different concentrations of PVP-K30. It can be seen the R_h of the reversed micelle in the presence of PVP-K30 has almost the same value as that in the absence of PVP-K30 when $\omega_0 < 17$; but with the increase of ω_0, the R_h in the presence of PVP-K30 is larger than that in the absence of it. This is because at small ω_0, the headgroup of AOT seized part of the water molecules in the PVP aqueous solution, which makes the PVP molecules more compact. While at higher ω_0, the effective hydrodynamic radius of the reversed micelle rises with the increase of PVP concentration. The AOT molecules arrange loosely with the increase of ω_0, so the hydrophobic part of the polymer may insert into the hydrophobic chains of the surfactant with the increase of the PVP concentration. The plot of R_h versus ω_0 in the absence of PVP-K30 is a straight line and agrees with the general expression for the radius of AOT reversed micelle [28].

Viscosities of the AOT reversed micelles in the presence of PVP-K30

The dependences of the specific viscosity (η_{sp}) and R_h of the reversed micelles on ω_0 are shown in Fig. 4. It is observed that the η_{sp} of the reversed micelle increases with the increase of ω_0. This is attributed to the larger size of the reversed micelle with the increase of ω_0, which leads to greater friction between the reversed micelles. Thus the viscosity of the system increases. This result is in agreement with the dynamic light scattering results (the plot inserted in Fig. 4).

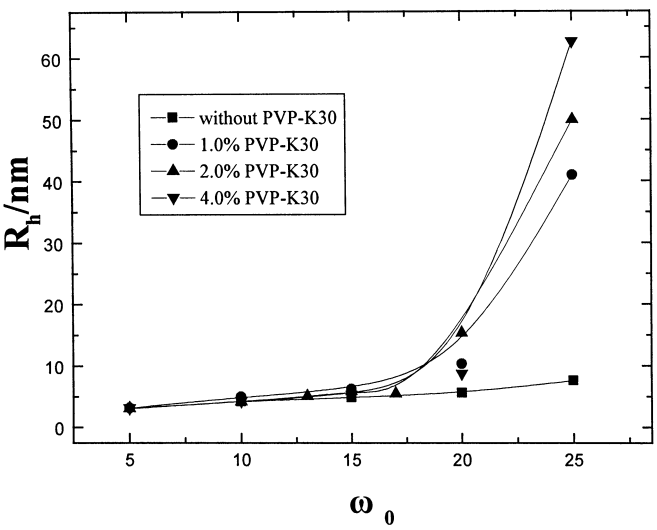

Fig. 3 Dependence of hydrodynamic radius (R_h) on ω_0 in the presence of different concentrations of PVP-K30

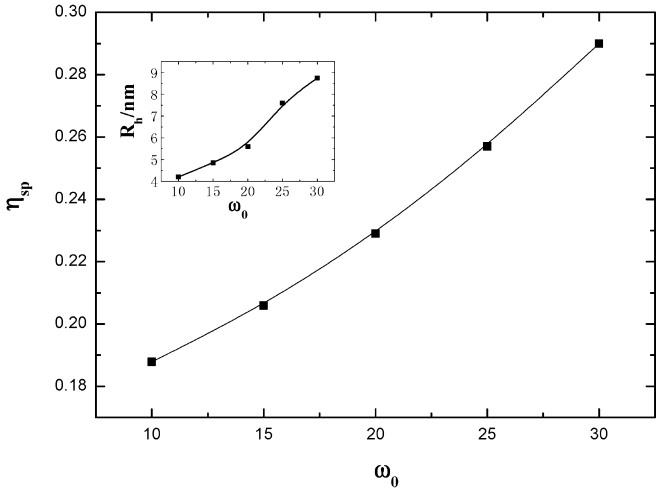

Fig. 4 Dependence of η_{sp} and R_h of water/AOT/heptane reversed micelles on ω_0

Figure 5 shows the dependence of the reduced viscosities of PVP-K30 and K90 aqueous solutions on their concentrations. The reduced viscosity of PVP-K90 solution increases more noticeably than that of the PVP-K30 solution. For example, the reduced viscosity of the PVP-K30 aqueous solution increases from 0.21 to 0.34 when W_P changes from 0.5%wt to 6.0%wt, while the PVP-K90 solution increases from 1.48 to 2.40 when W_P changes from 0.1%wt to 1.2%wt. The reason is that the larger molecules result in larger hydrodynamic volumes. Thus the entanglement between the intra- and intermolecules is stronger, which leads to the higher viscosity. Here, we also give the viscosities of the reversed micelles in the presence of the corresponding PVP content to its aqueous solution. The viscosity remains almost constant with the increase of W_{PVP} (shown in Fig. 6). This indicates that the size of the reversed micelles is almost unaffected by addition of PVP.

Table 1 shows the specific viscosity of the PVP aqueous solution and the reversed micelle at $\omega_0 = 5$ and $\omega_0 = 15$. It is shown that the specific viscosity of PVP-K30 is almost the same as that of PVP-K90 in the reversed micelle, while the specific viscosity of PVP-K30 in the aqueous solution is about one tenth of that of the PVP-K90 in the aqueous solution. The viscosity measured is the friction between the reversed micelles. This is in agreement with the DLS results that the effective radius of the reversed micelle remains almost constant at $\omega_0 = 15$. While the PVP molecules are stretched in the aqueous solution, thus the viscosity of PVP in the reversed micelle is much smaller than that in the aqueous solution.

According to Huggins equation,

$$\eta_{sp} \Big/ W_{PVP} = [\eta] + k[\eta]^2 W_{PVP} \quad (1)$$

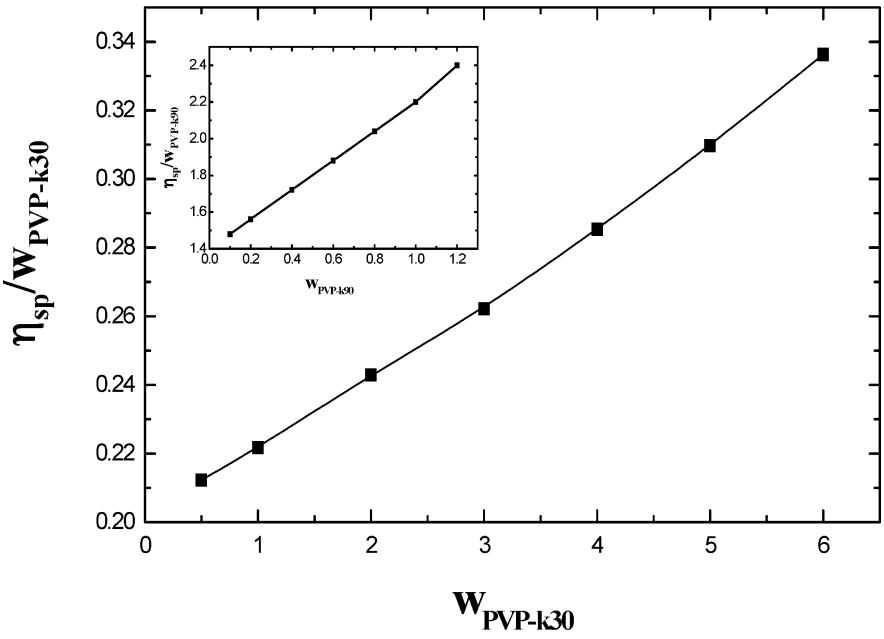

Fig. 5 Dependence of reduced viscosities of PVP-K30 and K90 on their concentrations in aqueous solutions

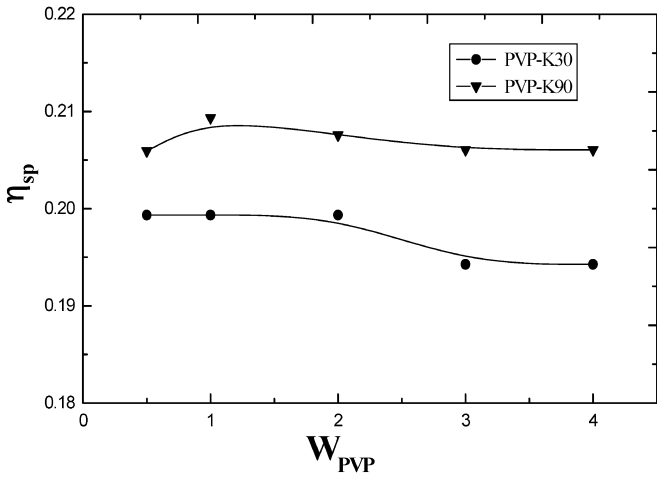

Fig. 6 Dependence of the specific viscosity of the reversed micelles ($\omega_0 = 15$) on W_{PVP}

The intrinsic viscosity of PVP-K30 and PVP-K90 are obtained by extrapolating the plot of η_{sp}/W_{PVP} versus W_{PVP} to $W_{PVP} = 0$ (Fig. 5). The intrinsic viscosities, $[\eta]$, of PVP-K30 and PVP-K90 are 0.202 and 1.4 g^{-1} dL, respectively. The molecular weight of PVP is obtained according to the following equation:

$$[\eta] = k_\eta M^\alpha \tag{2}$$

The molecular weight of PVP-K30 and PVP-K90 obtained are 3.0×10^4 and 5.2×10^5, respectively. The root-mean square of the end-to-end distance $[< r^2 >]^{1/2}$ of PVP-K30 and PVP-K90 can be obtained from the following equation [33]:

Table 1 Specific viscosities of PVP aqueous solutions ($W_{PVP} = 1.0\%$) and the AOT reverse micelles in the presence of PVP-K30 and PVP-K90 ($\omega_0 = 5$ and $\omega_0 = 15$)

PVP	Reversed micelles		Aqueous solution
	$\omega_0 = 5$	$\omega_0 = 15$	
K30	0.127	0.199	22.2
K90	0.133	0.208	220

$$[< r^2 >]^{1/2} = (M \times [\eta]/\phi)^{1/3} \tag{3}$$

where the value of ϕ is 2.1×10^{21} if the unit of $[\eta]$ is g^{-1} dL.

$[< r^2 >]^{1/2}$ of PVP-K30 and PVP-K90 are 14.24 nm and 70.25 nm, respectively.

The radius of the water core of the reversed micelle can be obtained according to the equation suggested by Kotlarchyk et al. [34]:

$$Rw = (3V_{H_2O}/A_S) \times \omega_0 + 3V_H/A_S \tag{4}$$

where V_{H_2O} is the volume of a single water molecule. A_S is the section area of the surfactant polar group. V_H is the hydration volume of the polar group.

The values of A_S and V_H obtained from reference [35] are 0.687 nm^2 and 0.311 nm^3, respectively. The radius of the water core of the reversed micelle at $\omega_0 = 5$ and $\omega_0 = 15$ are 2.01 nm and 3.32 nm, respectively. Thus, the $[< r^2 >]^{1/2}$ of these two PVP molecules is larger than the radius of the water core. At this low water content the polymer is too long to fit inside the water pool. PVP is a flexible molecule and can be solubilized in the reversed micelle as the structure shown in

Fig. 7. The AOT molecules array loosely due to the repulsive interactions between the polar headgroups of the surfactant. It is known that PVP is provided with a weak positive charge in water. Thus, the polar part of the PVP interacts with the headgroup of AOT molecule through electrostatic interaction, while the hydrophobic part of PVP can insert into the barrier layer of the reversed micelle. The larger difference between the viscosities of the aqueous solution and the reversed micelles suggests that the reversed micelles have a "crimple" action on the chain of the water-soluble polymer.

The effect of molecular weight on the Rh of the reversed micelle

Figure 3 shows that the R_h of the reversed micelle remains almost constant with the increase of $W_{PVP\text{-}K30}$ at $\omega_0 = 15$. In this section, the effect of molecular weight of PVP on the R_h of the AOT reversed micelle is investigated. Figure 8 shows the dependence of the R_h of the reversed micelle on the concentration of PVP-K30 and PVP-K90 at $\omega_0 = 15$. It is shown that the R_h of the reversed micelle remains almost constant with the increase of concentrations of both PVP-K30 and PVP-K90 at $\omega_0 = 15$. From the above calculation we know that the root-mean square of the end-to-end distance of PVP is larger than the size of the water pool. So, the PVP molecules can only be solubilized in the reversed micelle as shown in Fig. 7. It also can be seen from Fig. 8 that the R_h of the reversed micelle in the presence of PVP-K90 is a little larger than that in the presence of PVP-K30.

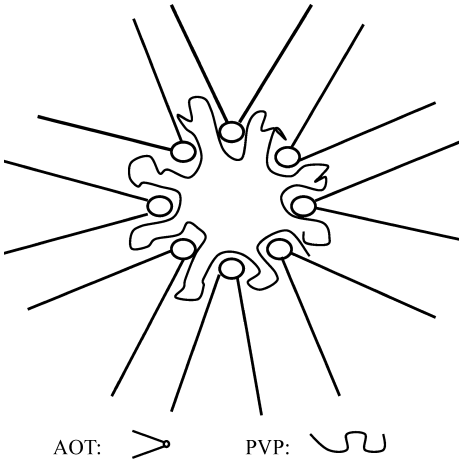

Fig. 7 Schematic structure of PVP molecules solubilized in the reversed micelle

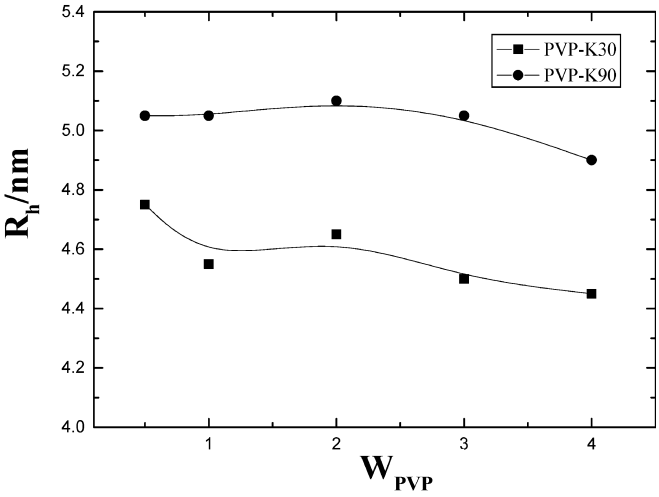

Fig. 8 Dependence of R_h on W_{PVP} in the AOT reversed micelle

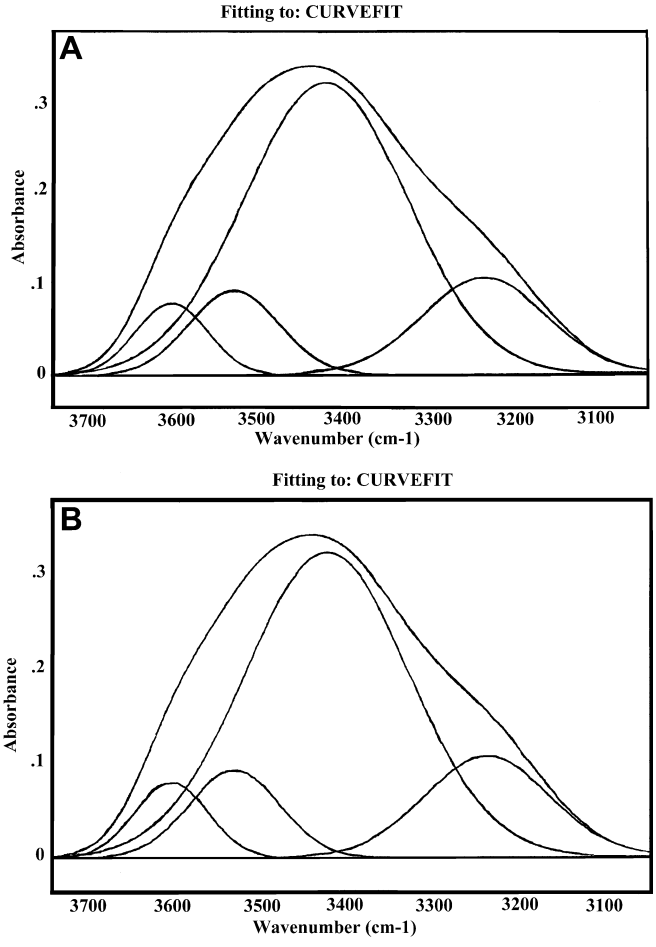

Fig. 9A–B Deconvolution of OH stretching vibration band of water contained in reversed micelles in the **A** absence and **B** presence of PVP-K30

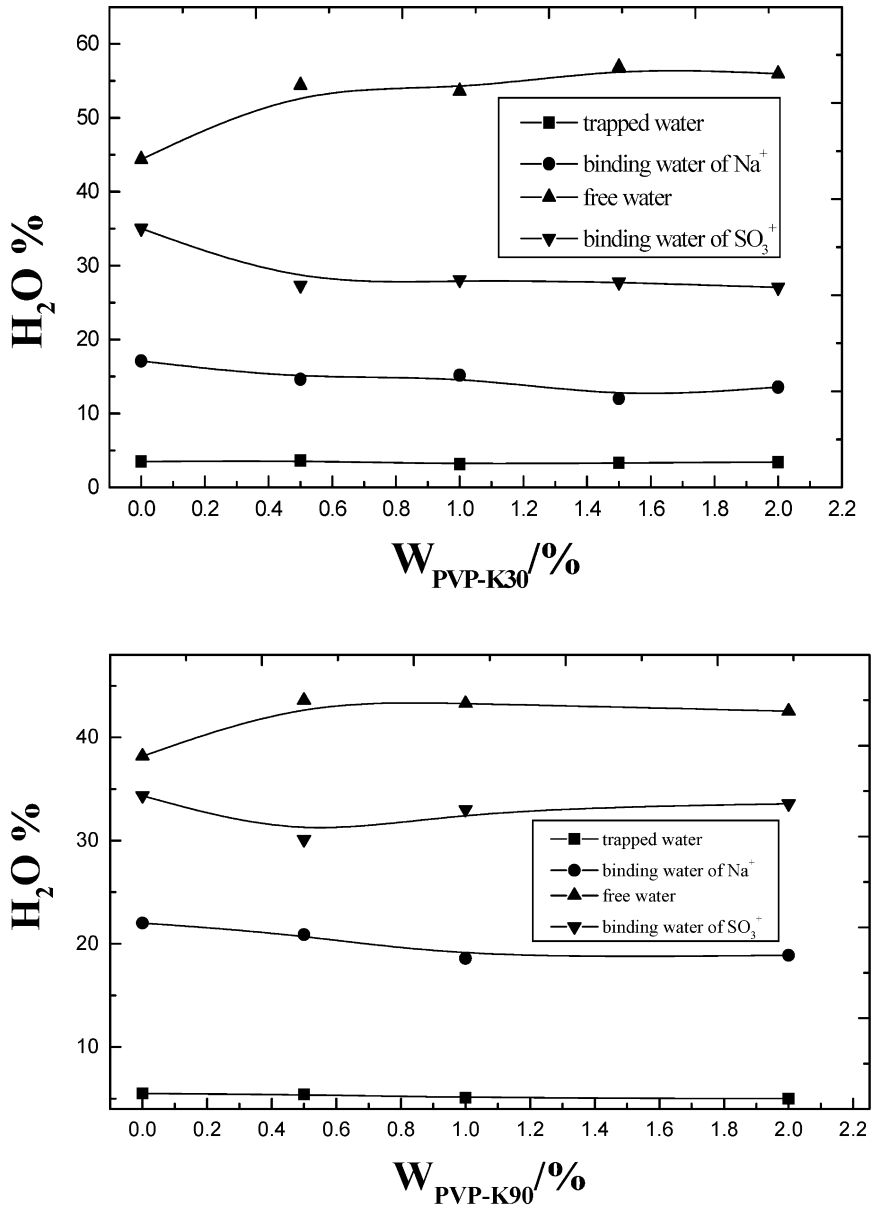

Fig. 10 Effect of PVP-K30 and PVP-K90 on the content of different kinds of water

The effect of PVP on the water state of the reversed micelle

The hydroxyl of the water in the reversed micelle systems can be resolved by the FTIR spectrum [12, 13, 36, 37]. Here we report the FTIR results of the water/AOT/heptane reversed micelle. The four sub-peaks at 3230 ± 10 cm^{-1}, 3420 ± 10 cm^{-1}, 3530 ± 10 cm^{-1}, and 3600 ± 10 cm^{-1} are shown in Fig. 9a. They are assigned to Na^+-bound water, bulk-like water, SO_3^--bound water, and trapped water, respectively. The bulk-like water refers to water in the water pool. It is similar to the bulky water and there are hydrogen bonds between the water molecules. Na^+-bound water and SO_3^--bound water refer to the water distributing around the polar head of the surfactant, namely the water binding to the sodium ion and the sulfonate ion. The trapped water refers to the water dispersing among the long hydrocarbon chains of surfactant molecules. These four kinds of water coexist in the reversed micelles and change to each other at nanosecond rates [38].

From Fig. 9b we can see that there are no obvious changes in the sub-peak positions after adding PVP-K30 to the reversed micelle at $\omega_0 = 15$. The contents of different water states are obtained according to reference [39] and listed in Fig. 10. It is seen that the contents of SO_3^--bound water and Na^+-bound water decrease, while the content of the bulk-like water increases, and the

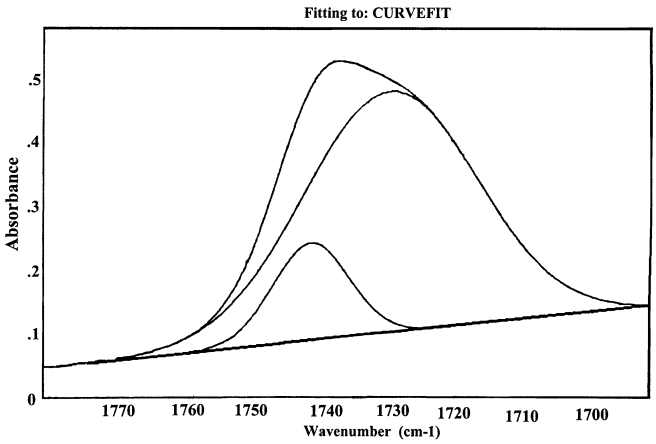

Fig. 11 Deconvoluted carbonyl stretch peak for the water/AOT/heptane system

content of the trapped water remains almost constant after adding PVP to the reversed micelle. Part of the water molecules released by the sodium ion and the sulfonate ion form a hydrogen bond with PVP,thus, the contents of SO_3^--bound water and Na^+-bound water decrease. When the remaining part of the water molecules come into the water pool, the content of the bulk-like water consequently increases.

The effect of PVP on the carbonyl of AOT in the reversed micelle

The carbonyl stretching of AOT is an antisymmetry peak. Two sub-peaks centering at 1740 and 1729 cm^{-1} are obtained by the deconvolution procedure, as shown in Fig. 11. These two sub-peaks correspond to the rotating isomers of the AOT molecules. The 1740 cm^{-1} and 1729 cm^{-1} sub-peaks correspond to the *trans* and the *cis* conformation of AOT molecules, respectively. According to the area of each peak over the total area, the content of each isomer can be obtained. The *trans* conformation of AOT is 85% of the total AOT, while the *cis* conformation of AOT is 15% by calculation. The peak position and the ratio of each peak area to their total area remain almost constant after adding PVP.

Conclusions

The phase diagrams of AOT dissolved in heptane in the presence and absence of PVP are investigated. Also, the interactions between PVP and the AOT reversed micelles are studied by means of measuring conductivity, viscosity, FTIR, and DLS. The following results are obtained:

1. The electrical conductivity of the reversed micelle initially increases, then decreases with the increase of ω_0; and the conductivity reaches its maximum value at $\omega_0 = 15$. The κ versus ω_0 plot of the reversed micelle in the presence of PVP is similar to that without PVP at $W_{PVP} \leq 2\%$, but $\omega_{0,max}$ becomes larger. The conductivity of the reversed micelle increases with the increase of ω_0 in the investigated range when W_{PVP} is over 4%.
2. The R_h of the reversed micelle both in the presence and absence of PVP increases with the increase of ω_0. The R_h versus ω_0 plot of the reversed micelle is a straight line. While the R_h of the reversed micelle in the presence of PVP initially increases slowly, it then rises rapidly with the increase of ω_0. The R_h also rises with the increase of PVP concentration when $\omega_0 > 17$. It is interesting to find that there is almost no effect of the PVP concentration on the R_h of the reversed micelle at $\omega_0 = 15$.
3. The reduced viscosity of the aqueous solution increases with the increase of PVP concentration, while that of the reversed micelle changes little, indicating that PVP is solubilized in the reversed micelle and that the reversed micelle has a "crimple" action on PVP molecules.
4. The content of different kinds of water is investigated by FTIR in the presence and absence of PVP. The results suggest that after adding PVP to the reversed micelle the contents of SO_3^--bound water and Na^+-bound water decrease, while the content of the bulk-like water increases, and the content of the trapped water remains almost constant.
5. Fourier deconvolution of C=O stretching bands of water/AOT/heptane reversed micelles shows two sub-peaks centering at 1740 and 1729 cm^{-1}, corresponding to the *trans* and *cis* conformation of AOT. It is observed that the carbonyl peak position, the *trans* and the *cis* conformation of AOT are not affected by PVP.

Aknowledgement The authors gratefully acknowledge financial support from National Natural Science Foundation (29973023) and National Microgravity Laboratory, Institute of Mechanics, CAS, Beijing, China.

References

1. Temsamani MB, Maeck M, Hassani IEI, Hurwitz HD (1998) J Phys Chem B 102:3335
2. Martin CA, Magid LJ (1981) J Phys Chem 85:3938
3. Casado J, Izquierdo C, Fuentes S, Moyá ML (1994) J Chem 71:446
4. Schulman JH, Stoeckenius W, Prince LM, (1959) J Phys Chem 63:1677
5. De TK, Maitra A, (1995) Adv Colloid Interface Sci 59:95
6. Pileni MP (1993) J Phys Chem 97:6961
7. Pileni MP (1993) Adv Colloid Interface Sci 46:139
8. Cui ZG, Yin FS (1999) Emulsifying technology and application. Light Industry Press of China, p 90
9. Haandrikman G, Daan GJR, Kerkhof FJM, Van Os NM, Rupert LAM (1992) J Phys Chem 96:9061
10. D'Angelo M, Onori G, Santucci A (1993) J Phys Chem 98:3189
11. Onori G, Santucci A (1993) J Phys Chem 97:5430
12. Li Q, Weng SF, Wu JG, Zhou NF (1998) J Phys Chem 102:3168
13. Li Q, Li T, Wu JG, Zhou NF (2000) J Colloid Interface Sci 229:298
14. Zhou NF, Li Q, Wu JG, Chen J, Weng SF, Xu GX (2001) Langmuir 17:4505
15. MacDonald H, Bedwell B, Gulari E, (1996) Langmuir 2:704
16. Jain TK, Varshney M, Maitra A, (1989) J Phys Chem 93:7409
17. González-Blanco C, Rodríguez LJ, Velázquez MM (1997) Langmuir 13:1938
18. Hou ZS, Li F, Wang HQ (2001) Colloid Polym Sci 279(1):8
19. Tamamusbi B, Watanabe N (1980) Colloid Polym Sci 258:174
20. Huang JS (1999) Langmuir 15:3718
21. Ikishima Y, Saito N, Arai M (1997) J Colloid Interface Sci 186:254
22. Hayes DG, Gulari E (1995) Langmuir 11:4695
23. Luan YX, Xu GY, Yuan SL, Xiao L, Zhang Z Q (2002) Langmuir 18:8700
24. Valstar A, Brown W, Almgren M (1999) Langmuir 15:2366
25. Xu GY, Zhang L, Mao HZ, Bao M, Lu Y (2001) Acta Phys Chim Sin 17:37 (in Chinese)
26. Meziani A, Touraud D, Zradba A, Clausse M, Kunz W (2000) J Mol Liquids 84:301
27. Filankembo A, André P, Lisiecki I, Petit C, Gulik-Krzywicki T, Ninham BW, Pileni MP (2000) Colloids Surf A: 174:221
28. César ATL, Wyn B, Mats A, Sílvia MBCosta (2000) Langmuir 16:465
29. Huruguen JP, Authier M, Greffe JL, Pileni PM (1991) Langmuir 7:243
30. Cassin G, Duda Y, Holovko M, Badiali JP, Pileni MP (1997) J Chem Phys 107:2683
31. Valstar A, Almgren M, Brown W (2000) Langmuir 16:922
32. Christoff M, Silveira N P, Samios D (2001) Langmuir 17:2885
33. Li ZM, Ye QM, Yang JP (1983) Macromol Comm 3:184 (in Chinese)
34. Kotlarchyk M (1982) J Phys Chem 86:3273
35. Liu K, Cruzan JD, Saykally RJ (1996) Science 271:929
36. Giammona G, Goffredi F, Liveri VT, Vassallo G (1992) J Colloid Interface Sci 154:411
37. Kitano H, Ichikawa K, Ide M, Fukuda M, Mizuno W (2001) Langmuir 17:1889
38. Hertz G (1975) In: Franks F (ed) Water—a comprehensive treatise, vol 3. Plenum Press, New York, chap 7
39. Xu GY, Zhang L, Yuang SL, Huang XR, Li GZ (2001) J Dispersion Sci Technol 22 (6):563